

This discussion paper is/has been under review for the journal Natural Hazards and Earth System Sciences (NHESD). Please refer to the corresponding final paper in NHESD if available.

A huge deep-seated ancient rock landslide: recognition, mechanism and stability

M. G. Tang^{1,2}, Q. Xu¹, Y. S. Li², R. Q. Huang¹, and G. Zheng¹

¹State Key Laboratory of Geohazard Prevention and Geoenvironment Protection, Chengdu University of Technology, No. 1 Erxianqiao Rd, 610059, Chengdu, China

²College of Environment and Civil Engineering, Chengdu University of Technology, No. 1 Erxianqiao Rd, 610059, Chengdu, China

Received: 17 September 2015 – Accepted: 21 September 2015
– Published: 5 November 2015

Correspondence to: Q. Xu (42604356@qq.com)

Published by Copernicus Publications on behalf of the European Geosciences Union.

NHESD

3, 6791–6844, 2015

A huge deep-seated ancient rock landslide

M. G. Tang et al.

[Title Page](#)

[Abstract](#)

[Introduction](#)

[Conclusions](#)

[References](#)

[Tables](#)

[Figures](#)

[⏪](#)

[⏩](#)

[◀](#)

[▶](#)

[Back](#)

[Close](#)

[Full Screen / Esc](#)

[Printer-friendly Version](#)

[Interactive Discussion](#)



Abstract

The identification of deep-seated landslides is a difficult problem and its failure mechanism is a research hotspot. This paper mainly discusses a very attractive huge deep-seated ancient landslide, it is a very good case to go further research.

About 15 years ago a large-scale abnormal geomorphology and geological phenomenon, containing a discontinuous stratum in output and color, was found in the new city of Fengjie, Three Gorges Project Reservoir, China. Two hypotheses for the interpretation of the abnormal phenomenon are a fault graben or a large-scale landslide. From then on continue collecting and analyzing relevant information, field investigation and test, now the results show that the fault graben, consisting of normal faults, could not have been formed under the north-south compressive structure stress of the local region. Meanwhile, a lot of unique geological features, interesting sliding trails and marks of the ancient landslide are discovered and identified in field and experiments. The deformation process and failure mechanism of the ancient landslide are clearly reappeared by a large centrifuge model experiment. Its failure mechanism can be analyzed as “creep-crack-cut”. The experiment strongly confirms that it is a huge deep-seated ancient rock landslide. And the failure precursor and key factors of rock slope are discussed. At last, the stability analysis shows that the landslide as a whole is stable and the secondary landslides at the front are basically stable. The results provide a technical support for decision making of the land use planning and construction of the new city, Fengjie.

1 Introduction

The identification and failure mechanism of deep-seated landslides is a hot spot subject (Crosta et al., 1996, 2000). In this paper discuss a very attractive huge deep-seated ancient landslide. The old city of Fengjie, Chongqing, China, would be inundated when the Three Gorges Project was completed in 2003. The Sanma Mountain, located

NHESSD

3, 6791–6844, 2015

A huge deep-seated ancient rock landslide

M. G. Tang et al.

[Title Page](#)

[Abstract](#)

[Introduction](#)

[Conclusions](#)

[References](#)

[Tables](#)

[Figures](#)

[⏪](#)

[⏩](#)

[◀](#)

[▶](#)

[Back](#)

[Close](#)

[Full Screen / Esc](#)

[Printer-friendly Version](#)

[Interactive Discussion](#)



upriver on the northern bank of the Yangtze River, was recommended as a site for the new city of Fengjie (Fig. 1). However, during the construction process, it was found that there is a large-scale abnormal phenomenon of geomorphology and geological structure. It contains a discontinuous stratum in output and color (Fig. 2). This strata discontinuity has been speculated to be the result of an ancient landslide (Wu, 1998; Nanjiang Geological Team, 1999) (Fig. 3). However, Li et al. (2002) put forward the hypothesis that it was caused by tectonic activity, and the surrounding area and the base of the body are cut by four normal faults (F8, F20, F19, and F26), that is to say it is a local fault graben (Fig. 4), and this idea was supported by Wang et al. (2006). We know that no matter the landslide or the tectonic activity can cause the phenomenon of a discontinuous stratum (Illies, 1981; Chang, 1981; Crosta et al., 1996, 2000; Cruden, 2007; John, 2012). Both above follow own scientific principles, but each other is easy to be misunderstood. Michael et al. (2012) found that the landslide scarp is easy to be misinterpreted as fault. On the other hand the tectonic activity can also play a key role on the development of large rock slope failures (Brideau, 2009). These two different hypotheses for the origin of the abnormal geological phenomenon caused confusion in land use planning and geological hazard prevention in the new city of Fengjie. This abnormal phenomenon of the strata discontinuity was caused by an ancient landslide or the tectonic activity? How to explain scientifically this natural phenomenon, failure mechanism and process? It need a lot of evidence and scientific analysis. In this paper, using field surveys, investigations of existing tunnels, deep drilling hole, research on the local tectonic setting and analysis on centrifuge model tests, a lot of geomorphic, structure evidence and sliding trace is found out, and it is confirmed that the fault graben consisting of normal faults could not have formed under the local region of north-south structure compressive stress. The result that it is a huge deep-seated ancient landslide and its failure mechanism of “creep-crack-cut” as a result of river rapidly incision into a nearly level layered slope with hard rock overlying soft rock.

A huge deep-seated ancient rock landslide

M. G. Tang et al.

[Title Page](#)[Abstract](#)[Introduction](#)[Conclusions](#)[References](#)[Tables](#)[Figures](#)[Back](#)[Close](#)[Full Screen / Esc](#)[Printer-friendly Version](#)[Interactive Discussion](#)

2 Geologic setting

We conducted field surveys and reviewed available geological maps, photographs and aerial photographs, papers and previous reports on the area (No. 107 Geological Team of Sichuan Province, 1980; Chen and Zhang, 1998). The regional setting of the area is summarized below.

2.1 Regional geological structure

Fengjie, in the Three Gorges Reservoir Area, is located at the eastern edge of the secondary terrain of China. It belongs to the Yangtze platform which contains basement rock mainly composed of early Proterozoic metamorphosed volcanoclastic rocks and intrusions of magmatic rocks. The overlying sedimentary rocks, which were deposited during the Triassic Period, were folded during uplift as part of the Yanshan Movement at the end of the Jurassic Period. As a result, secondary tectonic units, including the upper Yangtze platform fold belt, the marginal depression of the Sichuan Basin, and the Dabashan platform fold belt, were formed. These secondary tectonic units converge in Fengjie under compressive north-south stress (Figs. 5–7).

2.2 Strata and rocks

The rocks of the Sanma Mountain are sedimentary rocks of Triassic age (Fig. 7). The Jialingjiang Group (T_{1j}), which is of Early Triassic age, was deposited in shallow lagoon facies, and contains sedimentary limestone, dolomitic limestone, and marlite. These rocks occur in the core of the Zhuyi duplex inverted anticline. The Middle Triassic Badong Group (T_{2b}) was formed in inland lake and lagoon facies, with both clastic and carbonate deposition. The rocks making up the group consist of mudstone, silty mudstone, and marlite. The group is divided into units T_{2b}^1 to T_{2b}^5 . T_{2b}^1 to T_{2b}^4 occur in the new city of Fengjie.

NHESSD

3, 6791–6844, 2015

A huge deep-seated ancient rock landslide

M. G. Tang et al.

[Title Page](#)

[Abstract](#)

[Introduction](#)

[Conclusions](#)

[References](#)

[Tables](#)

[Figures](#)



[Back](#)

[Close](#)

[Full Screen / Esc](#)

[Printer-friendly Version](#)

[Interactive Discussion](#)



3 Fault graben can not form

The Zhuyi anticline at Sanma Mountain is a duplex inverted anticline (an overturned and closed fold, axial plane slanting, and overturned strata occur) (Figs. 7–9), and there is strong crumpling of strata in the core of the Zhuyi anticline (Figs. 7 (2), (3), (4) and 9). We investigated and measured the Zhuyi anticline tectonic stress field, the conjugate shear joint structural stress (Fig. 10) and the compression structural stress. The regional maximum principal stress direction is $344\text{--}352.5^\circ$ by means of stereographic projection analysis of occurrence of conjugate shear jointing and reversal stratum (Fig. 11). The result is the new city of Fengjie has a N-S compressive stress field as the tectonic background. The crust and mantle stresses and resulting rock deformation have resulted in closed fold and thrust compressional structures. The regional tectonic background is not consistent with formation of a graben structure under tensional stress. Under the control of N-S compressive stress, the geological structure in new city of Fengjie changed from potential strike-slip type in the early stage to potential thrust type during formation of the main structure.

In field we found that the four tension faults, F_8 , F_{20} , F_{19} , and F_{26} (Li Huizhong, 2002) (Fig. 4), share some common characteristics. The fault extension length is not long (F_8 : 1110 m, F_{19} : 150 m, F_{26} : 100 m), and the fault fracture zone width is not large (F_8 : 3.5 m, F_{19} : 0.1–1.1 m, F_{26} : 1–2 m; conversely, fault displacement is very large (F_8 : 150–180 m, F_{26} : 25–35 m). Studies have shown that the four normal faults, F_8 , F_{20} , F_{19} , and F_{26} (Li et al., 2002), did not form in a compressive stress field, according to geological mechanics (Illies, 1981; Chang et al., 1981). The footwall rock mass of the fault is preserved intact, although the hanging wall has almost entirely disintegrated; this observation is also not consistent with formation of a deep fault under confined conditions. The preserved thickness of T_{2b}^2 is only 200 m (Li Huizhong, 2002); a 300 m thickness of this formation has been lost as a result of faulting, which cannot have happened as part of normal faulting. Faults F_{20} and F_{26} cannot be observed on the ground, and faults F_8 and F_{19} show characteristics of sliding (pressure-shear), rather

A huge deep-seated ancient rock landslide

M. G. Tang et al.

[Title Page](#)

[Abstract](#)

[Introduction](#)

[Conclusions](#)

[References](#)

[Tables](#)

[Figures](#)



[Back](#)

[Close](#)

[Full Screen / Esc](#)

[Printer-friendly Version](#)

[Interactive Discussion](#)



Western lateral edge: there is a shallow groove called Longzibaogou leading into Yangjiaping gully (Fig. 18). Sliding scratches were observed during level drilling (Fig. 19).

The elevation of the slide tongue is about 90 m. The three secondary landslides at the foot of Sanmashan landslide are called as Houzishi, Zhiwuyou, and Laofangzi landslides.

4.2 Structural evidence

Based on regional geological mapping, drill holes, and a large excavation at the site, six engineering geological units were identified in the landslide. The units are as follows (Figs. 12 and 20):

The bedrock: (1) the third unit of the Middle Triassic Badong Group (T_{2b}^3). This unit contains gray or dark gray limestone and marlite, with a regional thickness of up to 205 m. (2) The second unit of the Badong Group, which consists of kermesinus or dark red-brown mudstone and silty mudstone, with a regional thickness of up to 550 m. (3) The first unit of the Badong Group. This unit consists of earthy yellow or light gray marlite and shale, with a regional thickness of about 70 m.

Artificial soil (Q^{mi}): the artificial soil is loose to dense, consists of clay and sand within crushed stone, and is randomly distributed on the landslide surface. The observed unit thickness is up to 10 m.

Alluvium (Q^{apl}): the alluvium is loose to less dense, sub-rounded to rounded gravel, cobbles, and boulders of mixed limestone and silty mudstone within sand, distributed at the front of landslide. The observed unit thickness is up to 15 m.

Landslide deposits (Q^{del}): including three units followed. (1) The first unit is dense to denser, and contains gray or dark gray crushed stone, within silty clay and sand. The crushed stone is derived from limestone and marlite (T_{2b}^3). A large foundation pit was constructed in the center of the landslide during field surveys (Figs. 21 and 22). The slide zone of the Zhiwuyou secondary landslide is exposed in the eastern wall (Figs. 23 and 24), and the rock masses in the western wall have anomalous attitudes

A huge deep-seated ancient rock landslide

M. G. Tang et al.

[Title Page](#)

[Abstract](#)

[Introduction](#)

[Conclusions](#)

[References](#)

[Tables](#)

[Figures](#)

[⏪](#)

[⏩](#)

[⏴](#)

[⏵](#)

[Back](#)

[Close](#)

[Full Screen / Esc](#)

[Printer-friendly Version](#)

[Interactive Discussion](#)



with respect to each other (Figs. 23 and 25). (2) The second unit is denser, reddish or dark red-brown, and contains crushed stone, within clay and silty clay. The crushed stone is derived from mudstone and silty mudstone (T_{2b}^2). (3) The third unit is denser, earthy yellow or light gray, and contains crushed stone, within sand and silty clay. The crushed stone is derived from limestone and shaly limestone (T_{2b}^1). The thickness of three units is up to 170 m.

5 Failure mechanism of the Sanmashan landslide

In order to research the deformation process and failure mechanism of the Sanmashan landslide, We carried out a large centrifuge model experiment. The centrifuge technology is widely applied in geotechnical and geological engineering, especially in the simulation of slope deformation and failure (Taylor, 1995; Nakajima, 2006).

5.1 Test device and principle

A centrifuge is a piece of equipment that puts an object in rotation around a fixed axis (spins it in a circle), applying a potentially strong force perpendicular to the axis of spin (outward). Geotechnical centrifuge modeling is used for physical testing of models involving soils and rock. Centrifuge acceleration is applied to scale models to scale the gravitational acceleration and enable prototype scale stresses to be obtained in scale models. Problems such as building and bridge foundations, earth dams, tunnels, and slope stability, including effects such as blast loading and earthquake shaking. Large centrifuges are used to simulate high gravity or acceleration environments. This experimental modeling used a centrifuge at the State Key Laboratory of Geohazard Prevention and Geoenvironment Protection in China (Fig. 26). Its maximum acceleration is 500 gt, and it is the largest geotechnical centrifuge in Asia.

It's mathematical description is similarity theory (Taylor, 1995). So according to the dimension relationship between geological model and experimental model, similarity

A huge deep-seated ancient rock landslide

M. G. Tang et al.

[Title Page](#)

[Abstract](#)

[Introduction](#)

[Conclusions](#)

[References](#)

[Tables](#)

[Figures](#)

[⏪](#)

[⏩](#)

[⏴](#)

[⏵](#)

[Back](#)

[Close](#)

[Full Screen / Esc](#)

[Printer-friendly Version](#)

[Interactive Discussion](#)



coefficient is deduced (Table 1). The geological model (Fig. 27) was generalized into a test model (Fig. 28). Rock parameters were obtained from physical and mechanical geotechnical engineering tests (Table 2).

5.2 Test result analysis

5 The experiment situations and observed results were as follows. First, there was a quiet period in which the Yangtze River cut into the central part of T_{2b}^3 . Tension cracking appeared at the surface of the slope, extending and scaling down (Figs. 27 and 29). Second, an intense period of incision in the bottom part of T_{2b}^3 occurred. Shear creep took place along the bottom weak zone, and there was rapid expansion of the upper
10 crack (Figs. 27 and 30). The third phase was a short and intense period of cutting into the bottom part of T_{2b}^2 . The crack cut through the bottom of the unit, and a landslide swiftly occurred (Figs. 27 and 31).

The deformation and failure mechanism can be summarized as “Creep–Crack–Cut” (Fig. 32). This failure mode generally occur as a result of river incision into a nearly
15 level layered slope with hard rock overlying soft rock. Such as the Chana landslide, Longyangxia in the Yellow River (Fig. 33) and the Yanchihe landslide of Hubei Province, China. In order to early recognition and warning of such landslides, key hazard factors and failure precursors of slope failure are discussed (Table 3).

6 Stability of the Sanmashan landslide

20 On the basis of the research above, we analyzed the seepage and stability of the Sanmashan deep-seated landslide using Geostudio 2007 (Fig. 34). The results of the analysis are discussed below.

If the reservoir water level increases from 145 to 175 m, using the current rate of reservoir scheduling, landslide stability will increase as a result of a rise in the
25 groundwater level behind the water level of the reservoir. After rising of the water

A huge deep-seated ancient rock landslide

M. G. Tang et al.

[Title Page](#)

[Abstract](#)

[Introduction](#)

[Conclusions](#)

[References](#)

[Tables](#)

[Figures](#)



[Back](#)

[Close](#)

[Full Screen / Esc](#)

[Printer-friendly Version](#)

[Interactive Discussion](#)



A huge deep-seated ancient rock landslide

M. G. Tang et al.

[Title Page](#)

[Abstract](#)

[Introduction](#)

[Conclusions](#)

[References](#)

[Tables](#)

[Figures](#)

[⏪](#)

[⏩](#)

[◀](#)

[▶](#)

[Back](#)

[Close](#)

[Full Screen / Esc](#)

[Printer-friendly Version](#)

[Interactive Discussion](#)



level of the reservoir to 175 m, landslide stability will begin to decrease with further rises in groundwater level. If the reservoir water level is reduced from 175 to 145 m, at the current rate of reservoir scheduling, the resulting decline in the groundwater level behind the water level of the reservoir will cause landslide stability to decrease. After reduction of the water level of the reservoir to 145 m, further decline of the groundwater level will cause landslide stability to increase gradually. (Fig. 35).

Considering the amount of rainfall (120 mm d^{-1} , 3 days) during the period when the reservoir water level changes from 175 to 145 m, and comparing with the situation with no rain, rainfall has little effect on the stability of the whole landslide, but has a large influence on the occurrence of secondary landslides at the front of the main slide. (Fig. 36).

At present, the stability coefficient of the Sanmashan landslide is greater than 1.20, and that of the secondary landslide at the front of the main slide is more than 1.076 before treatment.

7 Discussion

As is known to all, the geological phenomenon of a discontinuous stratum in output and color can be maybe interpreted as a fault graben or a large-scale landslide, but their genetic mechanism is different. In this paper the abnormal geologic body is a good case in the new city of Fengjie, Three Gorges Project Reservoir, China.

Firstly In order to find out the truth, the scientific method is that to prove whether it is contrary to the principle of geological mechanics. By means of survey analysis of geological structure stress and forming condition, we think that the fault graben consisting of four normal faults could not have formed under the local region of north-south compressive structure stress. Fengjie City, which is in the Three Gorges reservoir area, is located on the eastern edge of the secondary terrain of China. The region belongs to the Yangtze paraplatform, in which the basement rock is mainly composed of early Proterozoic metamorphic volcanoclastic rocks and magmatic

A huge deep-seated ancient rock landslide

M. G. Tang et al.

Title Page	
Abstract	Introduction
Conclusions	References
Tables	Figures
⏪	⏩
◀	▶
Back	Close
Full Screen / Esc	
Printer-friendly Version	
Interactive Discussion	



intrusions. The overlying sedimentary strata underwent folding during the Jurassic Yanshan Movement. As a result of the Yanshan Movement, secondary tectonic units were formed, including the upper Yangtze platform fold belt, the marginal depression of the Sichuan Basin, and the Dabashan platform fold belt. These secondary tectonic units converge in Fengjie under north-south compressive stress. Thus, the new city of Fengjie is sited at a special tectonic position. Sanma Mountain is located in the northern wing of the Zhuyi double reversal anticline. Under the influence of the N-S compressive stress field, deformation has mainly taken the form of closed-type folds and thrust compression structures, so the regional tectonic conditions are not suitable for formation of a fault graben. In addition, the hypothetical faults F_{20} and F_{26} cannot be observed in the field, while faults F_8 and F_{19} have the characteristics of sliding (pressure-shear) faults rather than those of normal faults. Thus, the interpretation of the geological anomaly as the fault graben is not supported by the available evidence.

Correspondingly, there is plenty of evidence to interpret as a landslide. In this paper the geomorphologic and geological features, subsurface geological units, and many sliding marks or trails of the Sanmashan landslide have been observed in the field. Especially the sliding marks and scrape around landslide is found, and their mechanical property is compressive. This is completely contrary to normal fault of a fault graben, because of their mechanical property is tensile. And the rockmass show their anomalous attitudes each other in the western wall of the foundation pit, this kind of geologic structure is only generated by landslides. The results of this study have confirmed that the Sanma Mountain in the new city of Fengjie is a large-scale ancient deep-seated landslide. From analysis of the slope deformation process and failure in centrifuge experiment model, it is reasonable to summarize the deformation and failure mechanism of landslide as “creep-crack-cut.” This type of failure generally occurs in a nearly level layered slope with overlying hard rock and underlying soft rock when rapid incision by a river takes place. Due to the limited level of the author, some of the phenomenon is not well presented, but it is a very attractive case to further research the huge deep-seated ancient landslide.

A huge deep-seated ancient rock landslide

M. G. Tang et al.

[Title Page](#)

[Abstract](#)

[Introduction](#)

[Conclusions](#)

[References](#)

[Tables](#)

[Figures](#)

[⏪](#)

[⏩](#)

[◀](#)

[▶](#)

[Back](#)

[Close](#)

[Full Screen / Esc](#)

[Printer-friendly Version](#)

[Interactive Discussion](#)



We also discussed landslide stability under increasing and decreasing of the reservoir water level, thinking reservoir scheduling at the current rate. Landslide stability will increase if the reservoir water level rises from 145 to 175 m, but landslide stability will decrease if the water level continues to rise above 175 m. Landslide stability will decrease if the reservoir water level drops from 175 to 145 m. Further water level decreases, to less than 145 m, will cause landslide stability to increase gradually. Rainfall has little impact on the stability of the whole landslide, but does have a great influence on the secondary landslide at the front of the main slide. At present, the landslide is stable as a whole; and the secondary landslide at the front is basically stable. But it needs to further research whether it can maintain long-term stability.

8 Conclusions

Using field surveys, investigation of existing tunnels, research into the tectonic setting, borehole drilling, and centrifuge model experiment, the result shows that the fault graben consisting of normal faults could not have been formed under the north-south compressive structure stress of the local region.

Meanwhile a lot of unique geological features and interesting sliding trails or marks of the ancient landslide are discovered or identified in field and experiment. It is proved that the abnormal geological phenomenon in the new city of Fengjie, Three Gorges Project Reservoir, China, is a large-scale ancient deep-seated landslide. The length of landslide is over 780 m, the width is about 1020 m, the maximum thickness is 170 m, the average thickness is about 125 m, and the volume is about 100 million m³. Three secondary landslides are present at the foot of the Sanmashan landslide: the Houzishi, Zhiwuyou, and Laofangzi landslides. It is summarized the deformation and failure mechanism of landslide as “creep-crack-cut.” And discuss the failure precursors and key factors, including the geological structure, boundary conditions, deformation and failure precursors, that can be refer to early recognition and warning of landslides.

At last, the stability analysis show that the landslide as a whole is stable and the secondary landslide at the front is basically stable. The results provide a technical support for decision making for the land use planning and construction of the new city of Fengjie. But there is a risk of local deformation and landslides because of the intensive construction and centrated population, So it is very necessary to draw up a strict land use plan.

**The Supplement related to this article is available online at
doi:10.5194/nhessd-3-6791-2015-supplement.**

Acknowledgement. This study was financially supported by the National Basic Research Program of China (973 Program; Grant No. 2013CB733202), the Key Project of TGR (Grant No.SXKY3-1-1-200901), the National Natural Science Foundation of China (Grant No. 41002111), and the State Key Laboratory of Geohazard Prevention and Geoenvironment Protection (SKLGP2009Z016). We thank Huang Xuebin, Xu Kaixiang and Cheng Wenming for their assistance sincerely. The manuscript was directed by Zhang Zhuoyuan, Li Lierong and Peng Guangzhong. Kai Wang contributed to centrifuge model. Zhang Wei, Xiao Ruihua, Zhang Lei, and others contributed to investigation and drilling. We also wish to thank the reviewers very much.

References

- Brideau, M., Yan, M., and Stead, D.: The role of tectonic damage and brittle rock fracture in the development of large rock slope failures, *Geomorphology*, 103, 30–49, 2009.
- Chang, W. Y., Li, Y. H., Ma, F. C., and Zhong, J. Y.: on the mechanical mechanism of the formation of graben, *Chinese Scientia Geologica Sinica*, 1, 1–11, 1981.
- Chen, M. S. and Zhang, S. H.: Characteristics and forming mechanism of opposite protruding arcuate structural zones in the Three Gorges Area of the Yangtze river, south China, *Geology and Mineral Resources of South China*, 1, 48–55, 1998.

A huge deep-seated ancient rock landslide

M. G. Tang et al.

[Title Page](#)

[Abstract](#)

[Introduction](#)

[Conclusions](#)

[References](#)

[Tables](#)

[Figures](#)

[⏪](#)

[⏩](#)

[◀](#)

[▶](#)

[Back](#)

[Close](#)

[Full Screen / Esc](#)

[Printer-friendly Version](#)

[Interactive Discussion](#)



**A huge deep-seated
ancient rock
landslide**M. G. Tang et al.

[Title Page](#)[Abstract](#)[Introduction](#)[Conclusions](#)[References](#)[Tables](#)[Figures](#)[⏪](#)[⏩](#)[◀](#)[▶](#)[Back](#)[Close](#)[Full Screen / Esc](#)[Printer-friendly Version](#)[Interactive Discussion](#)

- Crosta, G. B.: Landslide, spreading, deep-seated gravitational deformation: analysis, examples, problems and proposals, *Geografia Fisica e Dinamica Quaternaria*, 19, 297–313, 1996.
- Crosta, G. B. and Zanchi, A.: Deep-seated slope deformations: Huge, extraordinary, enigmatic phenomena, in: *Landslides in Research, Theory and Practice*, edited by: Bromhead E., Dixon N., and Ibsen M.-L., Thomas Telford, London, 351–358, 2000.
- Cruden, D. M. and Martin, C. D.: Before the Frank Slide, *Can. Geotech. J.*, 44, 765–780, 2007.
- GEO-SLOPE: Seepage Modeling with SEEP/W: User's Guide Version 6.16, GEO-SLOPE International, Calgary, AB, 2004.
- Glastonbury, J. and Fell, R.: Geotechnical characteristics of large rapid rock slides, *Can. Geotech. J.*, 47, 116–132, 2010.
- Huang, R. Q.: Mechanisms of large-scale landslides in China, *B. Eng. Geol. Environ.*, 71, 161–170, 2012.
- Illies, J. H.: Mechanism of garben formation, *Tectonophysics*, 73, 249–266, 1981.
- John, J. C. and Douglas, S.: *Landslides: Types, Mechanisms and Modeling*, Cambridge University Press, Cambridge, 2012.
- Li, H. L., Yi, S. H., and Deng, Q. L.: Development characteristics and their spatial variations of Badong formation in the Three Gorges Reservoir Region, *Journal of Eng. Geol.*, 14, 578–581, 2006.
- Li, H. Z., Zhou, Y., and Pan, Y. Z.: The stability analysis and protection measures of the Houzishi landslides in the Three Gorges Reservoir Region, *Hubei Geology & Mineral Resources*, 16, 97–104, 2002.
- Michael, W. H., Phillip, J. S., and Gregory, T. F.: When landslides are misinterpreted as faults: case studies from the Western United States, *Environ. Eng. Geosci.*, 11, 313–325, 2012.
- Nakajima, H. and Stadler, A. T.: Centrifuge modeling of one-step outflow tests for unsaturated parameter estimations, *Hydrol. Earth Syst. Sci.*, 10, 715–729, doi:10.5194/hess-10-715-2006, 2006.
- Nanjiang Geological Team: Investigation report of Sanmashan landslide in new Fengjie Town, Unpublished report, 1999 (in Chinese).
- No.107 Geological Team of Sichuan province: The regional geological report in Fengjie, China University of Geosciences, Wuhan, 1980.
- Sartori, M., Baillifard, F., Jaboyedoff, M., and Rouiller, J.-D.: Kinematics of the 1991 Randa rockslides (Valais, Switzerland), *Nat. Hazards Earth Syst. Sci.*, 3, 423–433, doi:10.5194/nhess-3-423-2003, 2003.

Taylor, R. N.: Centrifuges in Modeling: Principles and Scale Effects, Geotechnical Centrifuges Technology, edited by: Taylor, R. N., Blackie Academic and Professional, London, 19–33, 1995.

5 Wang, J. G., Zhou, Y., and Huang, Z. P.: Groundwater analyses of Houzishi landslide in the Three Gorges Reservoir, Chinese Journal of Rock Mechanics and Engineering, 25, 2757–2762, 2006.

Wu, F. Q.: Geological problems and suggestions on immigrant construction in some counties in Three Gorges Reservoir Region, Hydrogeology & Engineering Geology, 6, 44–46, 1998.

10 Zhang, Z. Y. and Huang, R. Q.: Epigenetic recreation of rockmass structure and time-dependent deformation, In: Proc of the 6th Congress of IAEG, Amsterdam, the Netherlands, A. A. Balkema Publishers, 2065–2072, 1990.

NHESSD

3, 6791–6844, 2015

A huge deep-seated ancient rock landslide

M. G. Tang et al.

[Title Page](#)

[Abstract](#)

[Introduction](#)

[Conclusions](#)

[References](#)

[Tables](#)

[Figures](#)

[⏪](#)

[▶⏩](#)

[◀](#)

[▶](#)

[Back](#)

[Close](#)

[Full Screen / Esc](#)

[Printer-friendly Version](#)

[Interactive Discussion](#)



A huge deep-seated ancient rock landslide

M. G. Tang et al.

[Title Page](#)

[Abstract](#)

[Introduction](#)

[Conclusions](#)

[References](#)

[Tables](#)

[Figures](#)

[⏪](#)

[⏩](#)

[◀](#)

[▶](#)

[Back](#)

[Close](#)

[Full Screen / Esc](#)

[Printer-friendly Version](#)

[Interactive Discussion](#)



Table 1. Key similarity coefficient in experimental model.

Physical quantity/Symbol	Unit	Similarity coefficient
Acceleration/ a	g	$N_a = 30$
Dimension/ L	m	$N_L = 1/3000$
Density/ ρ	g cm^{-3}	$N_\rho = 1$
Modulus/ E	Pa	$N_E = N_\rho N_a N_L = 1/100$
Internal friction angle/ φ	°	$N_\varphi = 1$
Cohesion/ c	Pa	$N_c = N_\rho N_a N_L = 1/100$
Poisson's ratio/ ν	–	$N_\nu = 1$

A huge deep-seated ancient rock landslide

M. G. Tang et al.

[Title Page](#)

[Abstract](#)

[Introduction](#)

[Conclusions](#)

[References](#)

[Tables](#)

[Figures](#)

⏪

⏩

◀

▶

[Back](#)

[Close](#)

[Full Screen / Esc](#)

[Printer-friendly Version](#)

[Interactive Discussion](#)



Table 2. Rock parameters in experimental model.

Rock	Modulus (MPa)	Poisson's ratio	Density (g cm^{-3})	Cohesion (KPa)	Internal friction angle ($^{\circ}$)
limestone T_{2b}^3	40–50	0.25 ~ 0.30	2.3–2.5	1.2	30–35
mudstone T_{2b}^2	8–10	0.35 ~ 0.40	2.1–2.3	5.0	20–25
marlite T_{2b}^1	20–30	0.30 ~ 0.35	2.2 ~ 2.4	3.0	28–35

A huge deep-seated ancient rock landslide

M. G. Tang et al.

Table 3. Key factors and precursors for reference to early recognition of slope failure.

Type of slope	Failure mechanism and type	Geological structure	Key factors Boundary conditions	Deformation	Failure precursor
layered slope	creep–crack–cut; deep seated rotational landslide	weak foundation or weak interlayer, common overlying limestone, dolomite, sandstone, slate and other hard rock; underlying mudstone, shale, coal and other soft rock; the dip angle is $8 \sim 20^\circ$ and incline to internal; $-\phi_r < \alpha < -\phi_p$	angle of the free surface slope $> 35^\circ$; the nose ridge, or both sides are gully or cracks and joints	depth of crack is 1/3 slope height, width of crack is up to 2 m	crack depth is up to 1/2 slope height, crack tend to be closed; the underlying soft rock cut out; the rock rupture infrasound constantly; spring at the foot of the slope; displacement rate $> 50 \text{ cm d}^{-1}$, deformation curve tangent angle is $85\text{--}90^\circ$, and the direction of displacement vector is uniform.

α is the weak plane angle, ϕ_r is the residual friction angle, ϕ_p is the basic friction angle.

[Title Page](#)

[Abstract](#) [Introduction](#)

[Conclusions](#) [References](#)

[Tables](#) [Figures](#)

[⏪](#) [⏩](#)

[◀](#) [▶](#)

[Back](#) [Close](#)

[Full Screen / Esc](#)

[Printer-friendly Version](#)

[Interactive Discussion](#)





Figure 1. Location of the new city of Fengjie in the Three Gorges reservoir area, China.

A huge deep-seated ancient rock landslide

M. G. Tang et al.

Title Page

Abstract

Introduction

Conclusions

References

Tables

Figures



Back

Close

Full Screen / Esc

Printer-friendly Version

Interactive Discussion



A huge deep-seated ancient rock landslide

M. G. Tang et al.

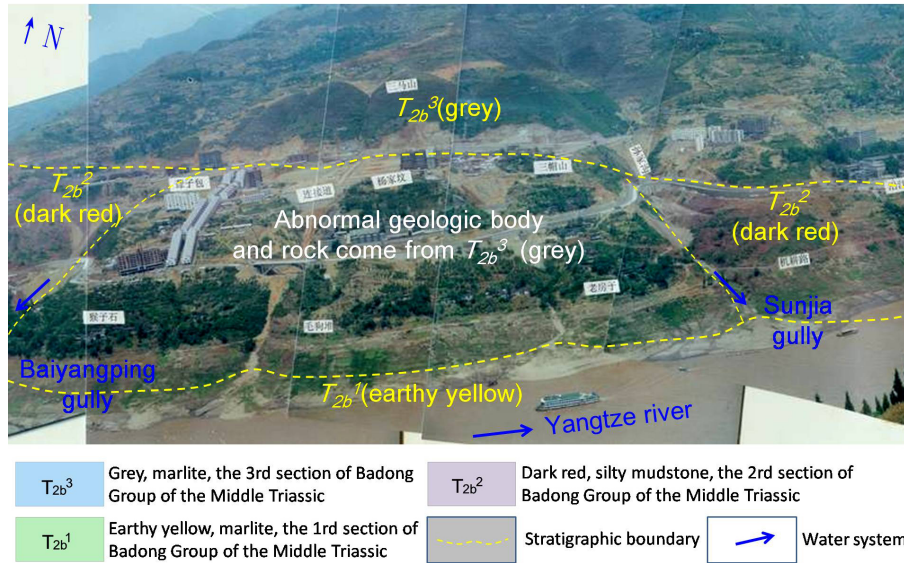


Figure 2. The abnormal geomorphologic and geological phenomenon at Sanma Mountain in the new city of Fengjie (photograph taken in 1998).

[Title Page](#)

[Abstract](#) [Introduction](#)

[Conclusions](#) [References](#)

[Tables](#) [Figures](#)

[◀](#) [▶](#)

[◀](#) [▶](#)

[Back](#) [Close](#)

[Full Screen / Esc](#)

[Printer-friendly Version](#)

[Interactive Discussion](#)



A huge deep-seated ancient rock landslide

M. G. Tang et al.

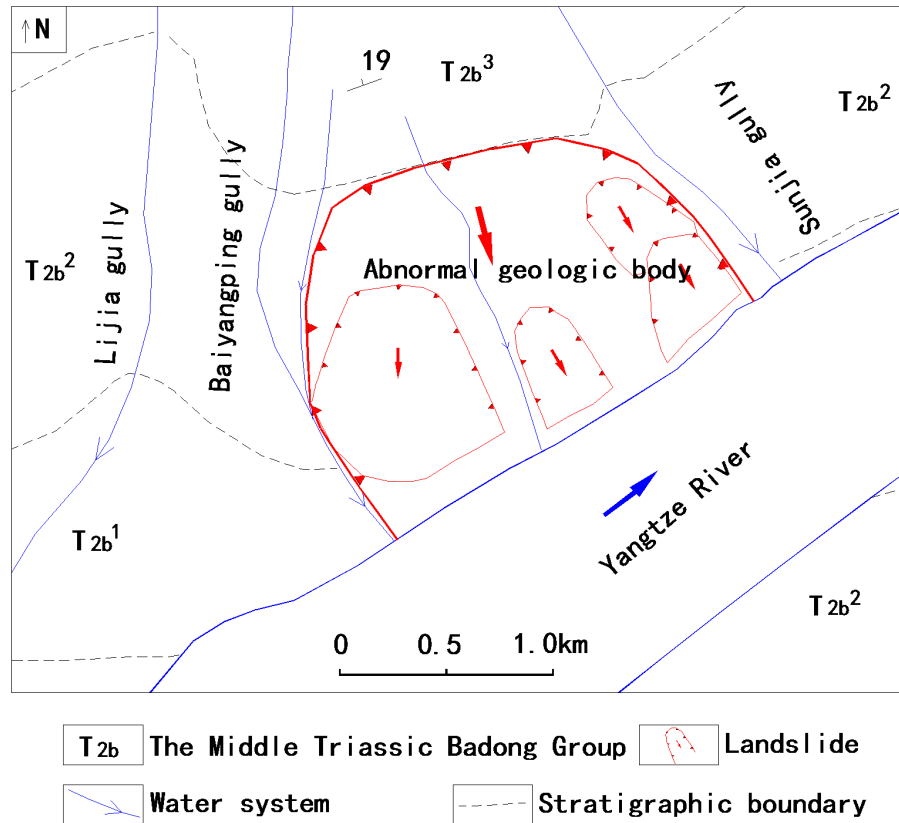


Figure 3. The abnormal geological phenomenon at Sanma Mountain speculated as a landslide.

[Title Page](#)

[Abstract](#)

[Introduction](#)

[Conclusions](#)

[References](#)

[Tables](#)

[Figures](#)

[◀](#)

[▶](#)

[◀](#)

[▶](#)

[Back](#)

[Close](#)

[Full Screen / Esc](#)

[Printer-friendly Version](#)

[Interactive Discussion](#)



A huge deep-seated ancient rock landslide

M. G. Tang et al.

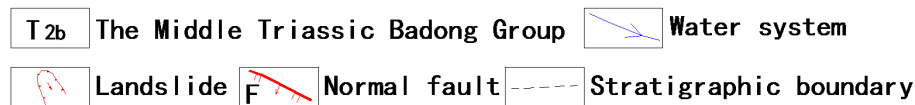
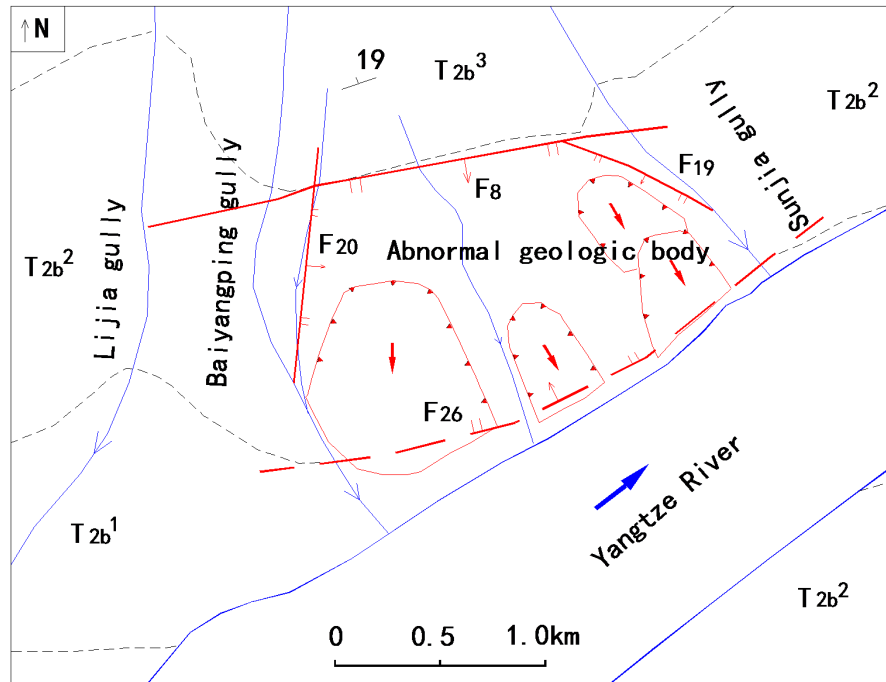


Figure 4. The abnormal geological phenomenon at Sanma Mountain explained as a fault graben (Li et al., 2002).

[Title Page](#)

[Abstract](#)

[Introduction](#)

[Conclusions](#)

[References](#)

[Tables](#)

[Figures](#)

[⏪](#)

[⏩](#)

[◀](#)

[▶](#)

[Back](#)

[Close](#)

[Full Screen / Esc](#)

[Printer-friendly Version](#)

[Interactive Discussion](#)



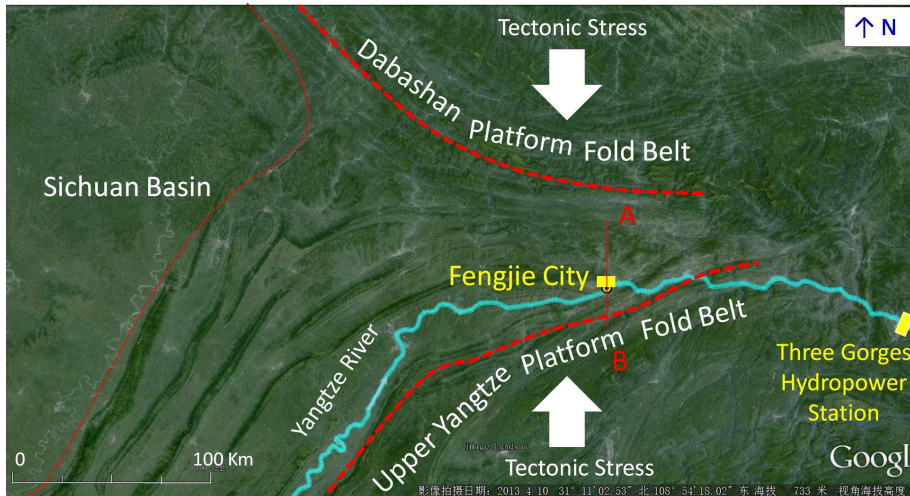


Figure 5. Outline of regional tectonics and stress.

A huge deep-seated ancient rock landslide

M. G. Tang et al.

Title Page	
Abstract	Introduction
Conclusions	References
Tables	Figures
◀	▶
◀	▶
Back	Close
Full Screen / Esc	
Printer-friendly Version	
Interactive Discussion	



A huge deep-seated ancient rock landslide

M. G. Tang et al.

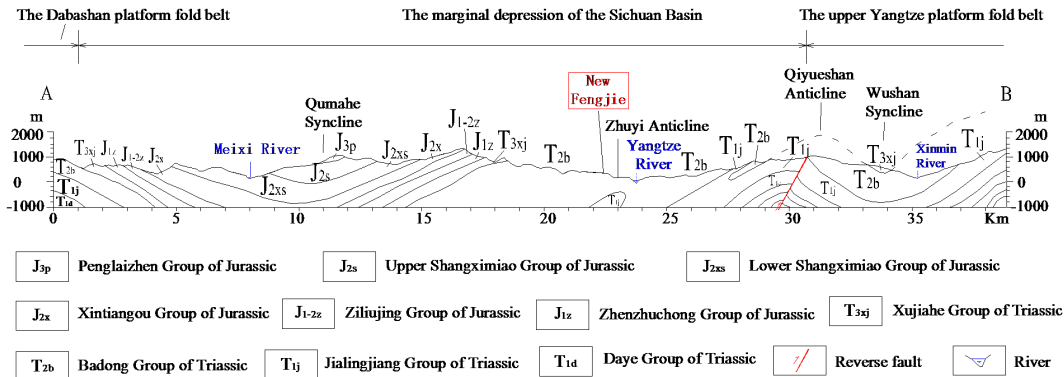


Figure 6. Cross section outline of regional tectonics and stress.

[Title Page](#)

[Abstract](#) [Introduction](#)

[Conclusions](#) [References](#)

[Tables](#) [Figures](#)

[⏪](#) [⏩](#)

[⏴](#) [⏵](#)

[Back](#) [Close](#)

[Full Screen / Esc](#)

[Printer-friendly Version](#)

[Interactive Discussion](#)



A huge deep-seated ancient rock landslide

M. G. Tang et al.

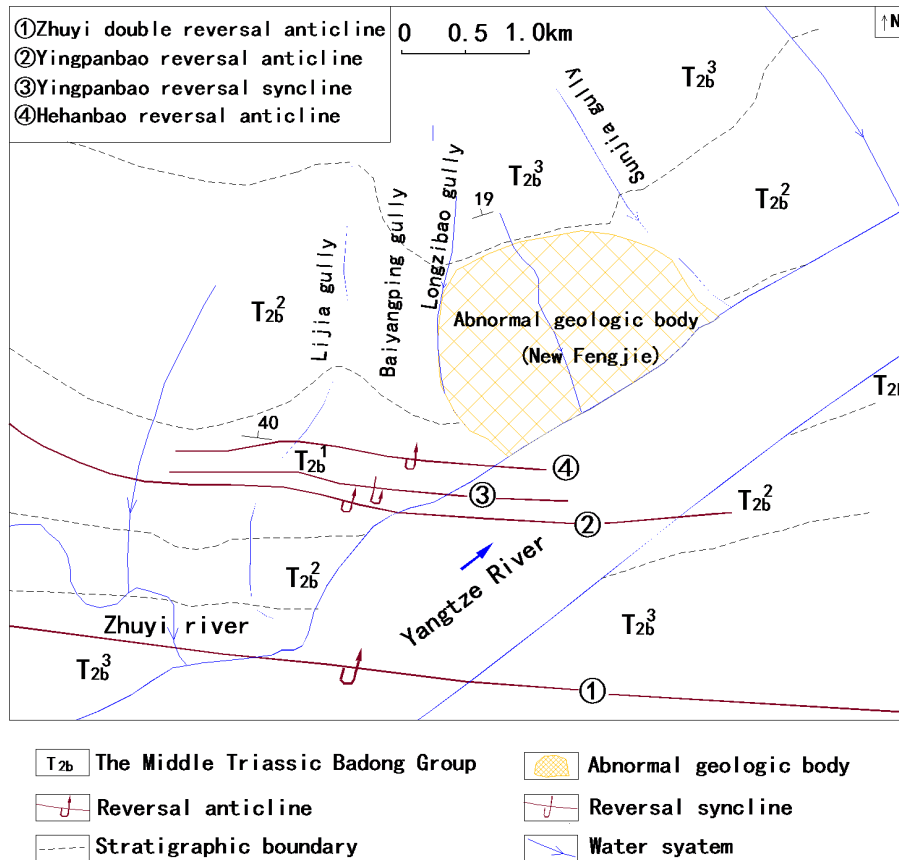


Figure 7. Outline geological map of the new city of Fengjie.

Discussion Paper | Discussion Paper | Discussion Paper | Discussion Paper | Discussion Paper | Discussion Paper | Discussion Paper | Discussion Paper

Title Page

Abstract

Introduction

Conclusions

References

Tables

Figures

◀

▶

◀

▶

Back

Close

Full Screen / Esc

Printer-friendly Version

Interactive Discussion



A huge deep-seated ancient rock landslide

M. G. Tang et al.

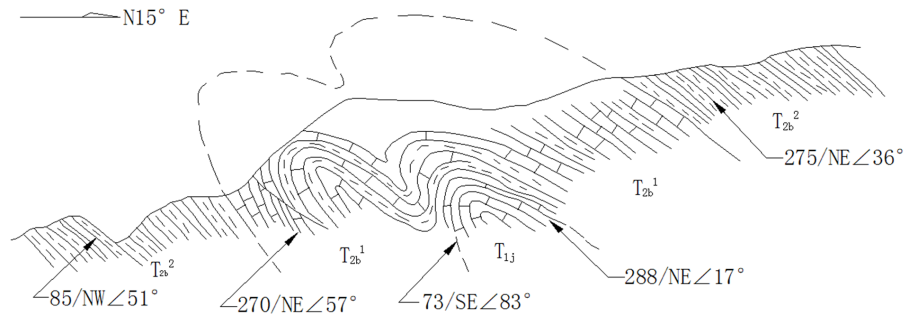


Figure 8. The geological profile of a duplex inverted anticline in the core of the Zhuyi anticline.

[Title Page](#)

[Abstract](#)

[Introduction](#)

[Conclusions](#)

[References](#)

[Tables](#)

[Figures](#)



[Back](#)

[Close](#)

[Full Screen / Esc](#)

[Printer-friendly Version](#)

[Interactive Discussion](#)





Figure 9. Ripples displaying reversal rock.

A huge deep-seated ancient rock landslide

M. G. Tang et al.

[Title Page](#)

[Abstract](#)

[Introduction](#)

[Conclusions](#)

[References](#)

[Tables](#)

[Figures](#)

[◀](#)

[▶](#)

[◀](#)

[▶](#)

[Back](#)

[Close](#)

[Full Screen / Esc](#)

[Printer-friendly Version](#)

[Interactive Discussion](#)



A huge deep-seated ancient rock landslide

M. G. Tang et al.



Figure 10. Conjugate shear jointing.

[Title Page](#)

[Abstract](#)

[Introduction](#)

[Conclusions](#)

[References](#)

[Tables](#)

[Figures](#)



[Back](#)

[Close](#)

[Full Screen / Esc](#)

[Printer-friendly Version](#)

[Interactive Discussion](#)



A huge deep-seated ancient rock landslide

M. G. Tang et al.

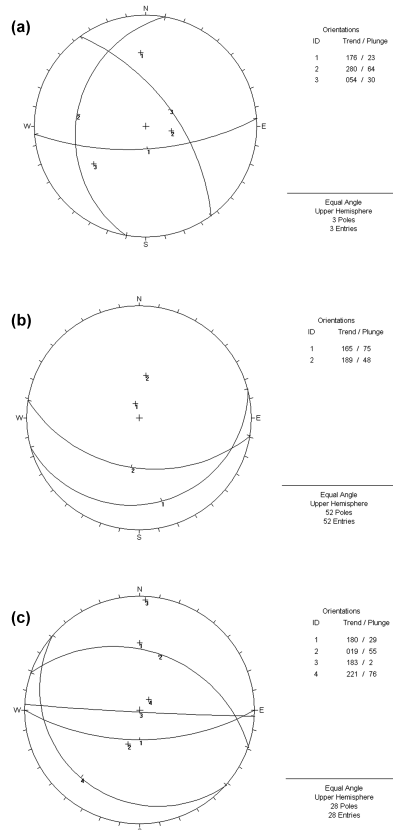


Figure 11. Stereographic projection analysis. **(a)** Occurrence of conjugate shear jointing. **(b)** Occurrence of stratum in the north wing. **(c)** Occurrence of stratum in the south wing.

[Title Page](#)
[Abstract](#) [Introduction](#)
[Conclusions](#) [References](#)
[Tables](#) [Figures](#)
⏪ ⏩
◀ ▶
[Back](#) [Close](#)
[Full Screen / Esc](#)
[Printer-friendly Version](#)
[Interactive Discussion](#)



A huge deep-seated ancient rock landslide

M. G. Tang et al.

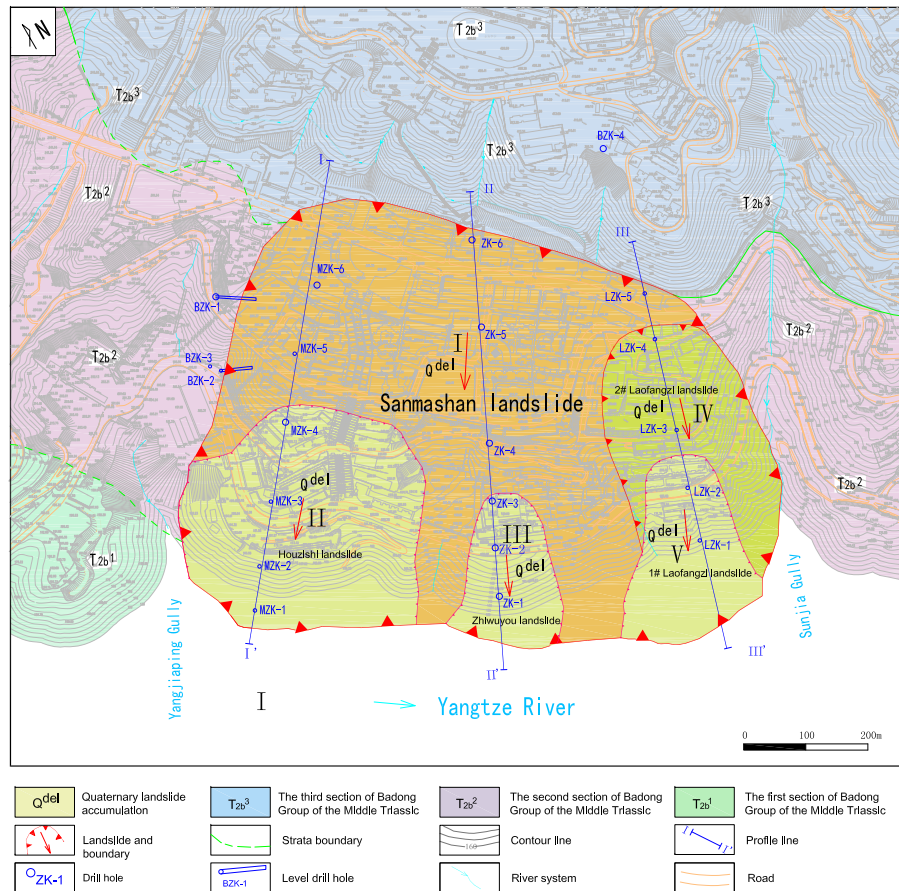


Figure 12. The geological map of the Sanmashan landslide (topographic map in October 2002).

Title Page

Abstract

Introduction

Conclusions

References

Tables

Figures



Back

Close

Full Screen / Esc

Printer-friendly Version

Interactive Discussion



A huge deep-seated ancient rock landslide

M. G. Tang et al.

[Title Page](#)

[Abstract](#)

[Introduction](#)

[Conclusions](#)

[References](#)

[Tables](#)

[Figures](#)



[Back](#)

[Close](#)

[Full Screen / Esc](#)

[Printer-friendly Version](#)

[Interactive Discussion](#)

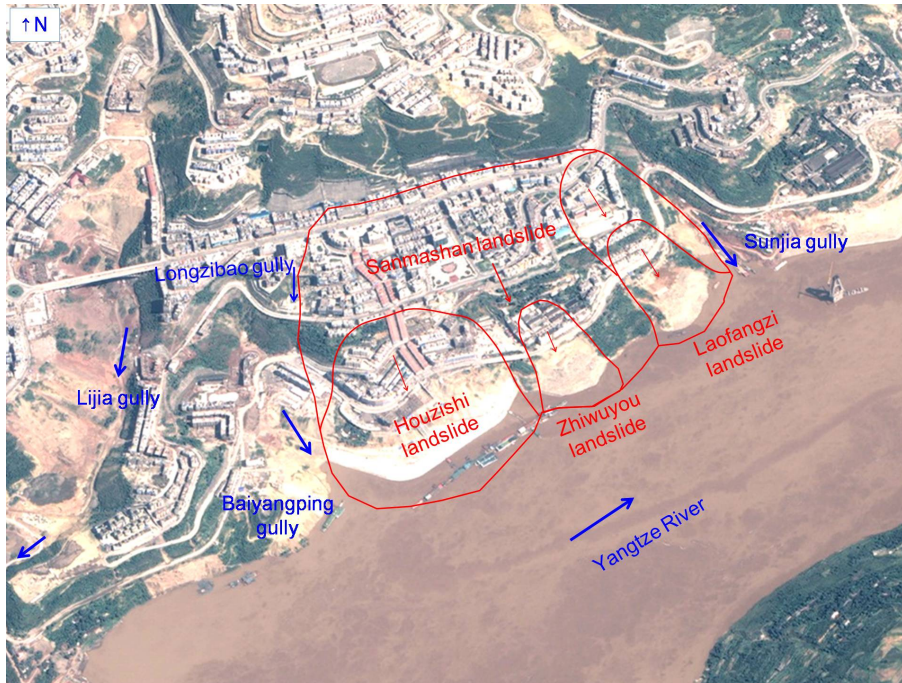


Figure 13. The remote image of the Sanmashan landslide (Satellite image in September 2004).



Figure 14. The scarp of the Sanmashan landslide (March 2006).

A huge deep-seated ancient rock landslide

M. G. Tang et al.

[Title Page](#)

[Abstract](#)

[Introduction](#)

[Conclusions](#)

[References](#)

[Tables](#)

[Figures](#)

[◀](#)

[▶](#)

[◀](#)

[▶](#)

[Back](#)

[Close](#)

[Full Screen / Esc](#)

[Printer-friendly Version](#)

[Interactive Discussion](#)





Figure 15. The sliding scarp of the scarp be revealed by foundation excavation.

A huge deep-seated ancient rock landslide

M. G. Tang et al.

[Title Page](#)

[Abstract](#)

[Introduction](#)

[Conclusions](#)

[References](#)

[Tables](#)

[Figures](#)



[Back](#)

[Close](#)

[Full Screen / Esc](#)

[Printer-friendly Version](#)

[Interactive Discussion](#)





Figure 16. The eastern lateral edge of the Sanmashan landslide.

A huge deep-seated ancient rock landslide

M. G. Tang et al.

[Title Page](#)

[Abstract](#)

[Introduction](#)

[Conclusions](#)

[References](#)

[Tables](#)

[Figures](#)

[⏪](#)

[⏩](#)

[◀](#)

[▶](#)

[Back](#)

[Close](#)

[Full Screen / Esc](#)

[Printer-friendly Version](#)

[Interactive Discussion](#)





Figure 17. The sliding zone and slip mass in tunnel near by the eastern lateral edge.

A huge deep-seated ancient rock landslide

M. G. Tang et al.

[Title Page](#)

[Abstract](#)

[Introduction](#)

[Conclusions](#)

[References](#)

[Tables](#)

[Figures](#)

[◀](#)

[▶](#)

[◀](#)

[▶](#)

[Back](#)

[Close](#)

[Full Screen / Esc](#)

[Printer-friendly Version](#)

[Interactive Discussion](#)





Figure 18. The western lateral edge of the Sanmashan landslide.

A huge deep-seated ancient rock landslide

M. G. Tang et al.

[Title Page](#)

[Abstract](#)

[Introduction](#)

[Conclusions](#)

[References](#)

[Tables](#)

[Figures](#)



[Back](#)

[Close](#)

[Full Screen / Esc](#)

[Printer-friendly Version](#)

[Interactive Discussion](#)



A huge deep-seated ancient rock landslide

M. G. Tang et al.



Figure 19. The sliding scarp in level drill hole near by the western lateral edge.

[Title Page](#)[Abstract](#)[Introduction](#)[Conclusions](#)[References](#)[Tables](#)[Figures](#)[◀](#)[▶](#)[◀](#)[▶](#)[Back](#)[Close](#)[Full Screen / Esc](#)[Printer-friendly Version](#)[Interactive Discussion](#)

A huge deep-seated ancient rock landslide

M. G. Tang et al.

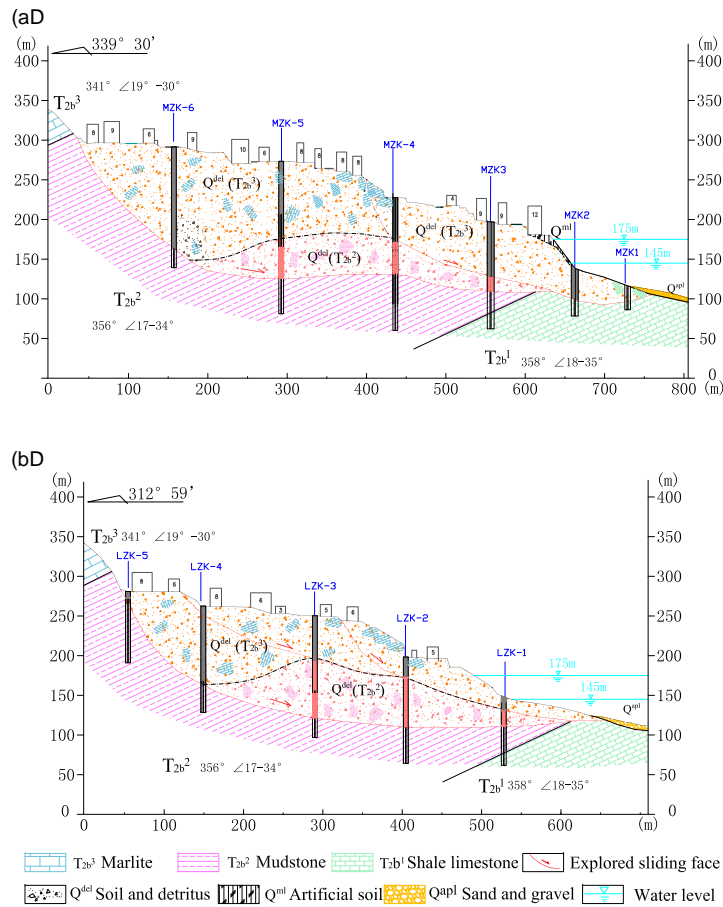


Figure 20. The geological profile of the Sanmashan landslide. **(a)** Section of I-I'. **(b)** Section of III-III'



A huge deep-seated ancient rock landslide

M. G. Tang et al.

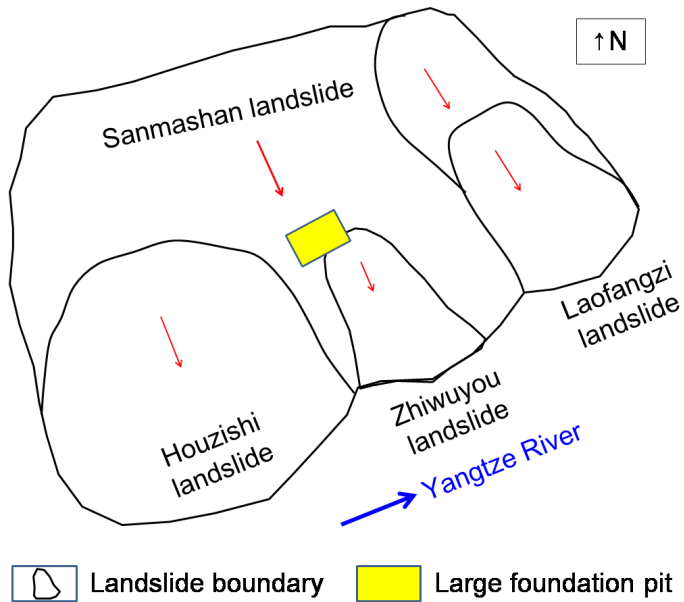


Figure 21. Location of the large foundation pit in the center of the landslide.

Title Page

Abstract

Introduction

Conclusions

References

Tables

Figures



Back

Close

Full Screen / Esc

Printer-friendly Version

Interactive Discussion





Figure 22. Overview of the foundation pit (photograph taken in 2013).

A huge deep-seated ancient rock landslide

M. G. Tang et al.

[Title Page](#)

[Abstract](#)

[Introduction](#)

[Conclusions](#)

[References](#)

[Tables](#)

[Figures](#)

[◀](#)

[▶](#)

[◀](#)

[▶](#)

[Back](#)

[Close](#)

[Full Screen / Esc](#)

[Printer-friendly Version](#)

[Interactive Discussion](#)



A huge deep-seated ancient rock landslide

M. G. Tang et al.

[Title Page](#)

[Abstract](#)

[Introduction](#)

[Conclusions](#)

[References](#)

[Tables](#)

[Figures](#)



[Back](#)

[Close](#)

[Full Screen / Esc](#)

[Printer-friendly Version](#)

[Interactive Discussion](#)



Figure 23. The geologic structure of four walls in the foundation pit.

A huge deep-seated ancient rock landslide

M. G. Tang et al.



Figure 24. Close-up view of the slide zone of the Zhiwuyou secondary landslide.

[Title Page](#)

[Abstract](#)

[Introduction](#)

[Conclusions](#)

[References](#)

[Tables](#)

[Figures](#)



[Back](#)

[Close](#)

[Full Screen / Esc](#)

[Printer-friendly Version](#)

[Interactive Discussion](#)





Figure 25. Rockmass showing their anomalous attitudes each other in the western wall of the foundation pit, and this kind of geologic structure is only generated by landslides.

A huge deep-seated ancient rock landslide

M. G. Tang et al.

[Title Page](#)

[Abstract](#)

[Introduction](#)

[Conclusions](#)

[References](#)

[Tables](#)

[Figures](#)

[◀](#)

[▶](#)

[◀](#)

[▶](#)

[Back](#)

[Close](#)

[Full Screen / Esc](#)

[Printer-friendly Version](#)

[Interactive Discussion](#)



A huge deep-seated ancient rock landslide

M. G. Tang et al.

[Title Page](#)

[Abstract](#)

[Introduction](#)

[Conclusions](#)

[References](#)

[Tables](#)

[Figures](#)



[Back](#)

[Close](#)

[Full Screen / Esc](#)

[Printer-friendly Version](#)

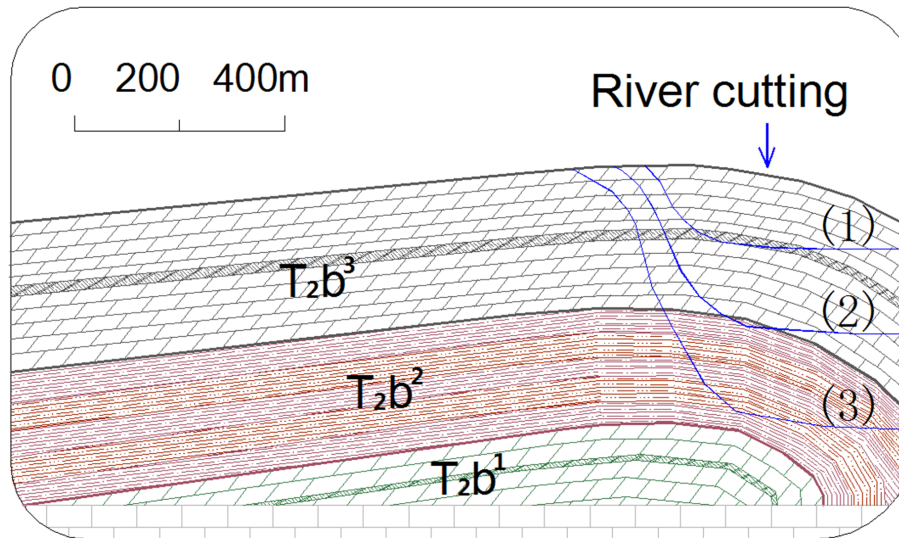
[Interactive Discussion](#)



Figure 26. The geotechnical centrifuge used in experimental modeling.

A huge deep-seated ancient rock landslide

M. G. Tang et al.

[Title Page](#)[Abstract](#)[Introduction](#)[Conclusions](#)[References](#)[Tables](#)[Figures](#)[◀](#)[▶](#)[◀](#)[▶](#)[Back](#)[Close](#)[Full Screen / Esc](#)[Printer-friendly Version](#)[Interactive Discussion](#)**Figure 27.** The geological model of slope.

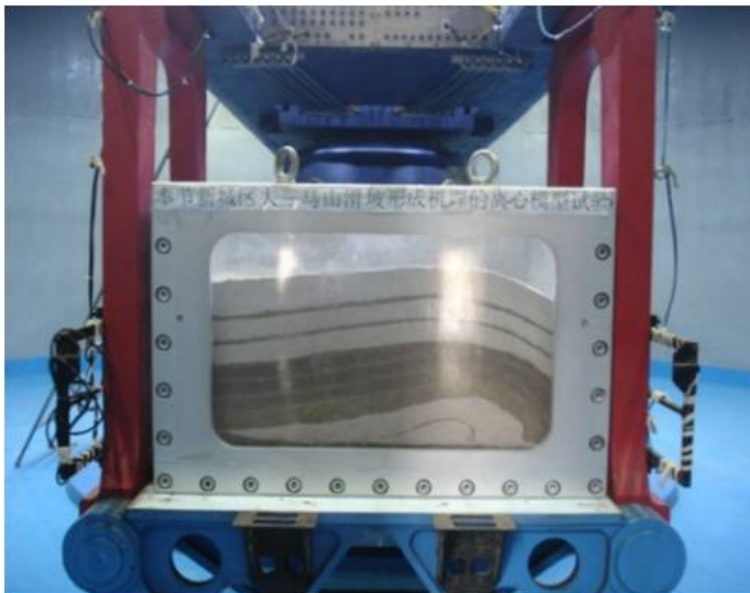


Figure 28. The experimental model.

A huge deep-seated ancient rock landslide

M. G. Tang et al.

[Title Page](#)

[Abstract](#)

[Introduction](#)

[Conclusions](#)

[References](#)

[Tables](#)

[Figures](#)



[Back](#)

[Close](#)

[Full Screen / Esc](#)

[Printer-friendly Version](#)

[Interactive Discussion](#)





Figure 29. Tension cracking in trailing edge and top.

A huge deep-seated ancient rock landslide

M. G. Tang et al.

[Title Page](#)

[Abstract](#)

[Introduction](#)

[Conclusions](#)

[References](#)

[Tables](#)

[Figures](#)

[◀](#)

[▶](#)

[◀](#)

[▶](#)

[Back](#)

[Close](#)

[Full Screen / Esc](#)

[Printer-friendly Version](#)

[Interactive Discussion](#)





Figure 30. Going cracking and shear creeping at the bottom.

A huge deep-seated ancient rock landslide

M. G. Tang et al.

[Title Page](#)

[Abstract](#)

[Introduction](#)

[Conclusions](#)

[References](#)

[Tables](#)

[Figures](#)



[Back](#)

[Close](#)

[Full Screen / Esc](#)

[Printer-friendly Version](#)

[Interactive Discussion](#)



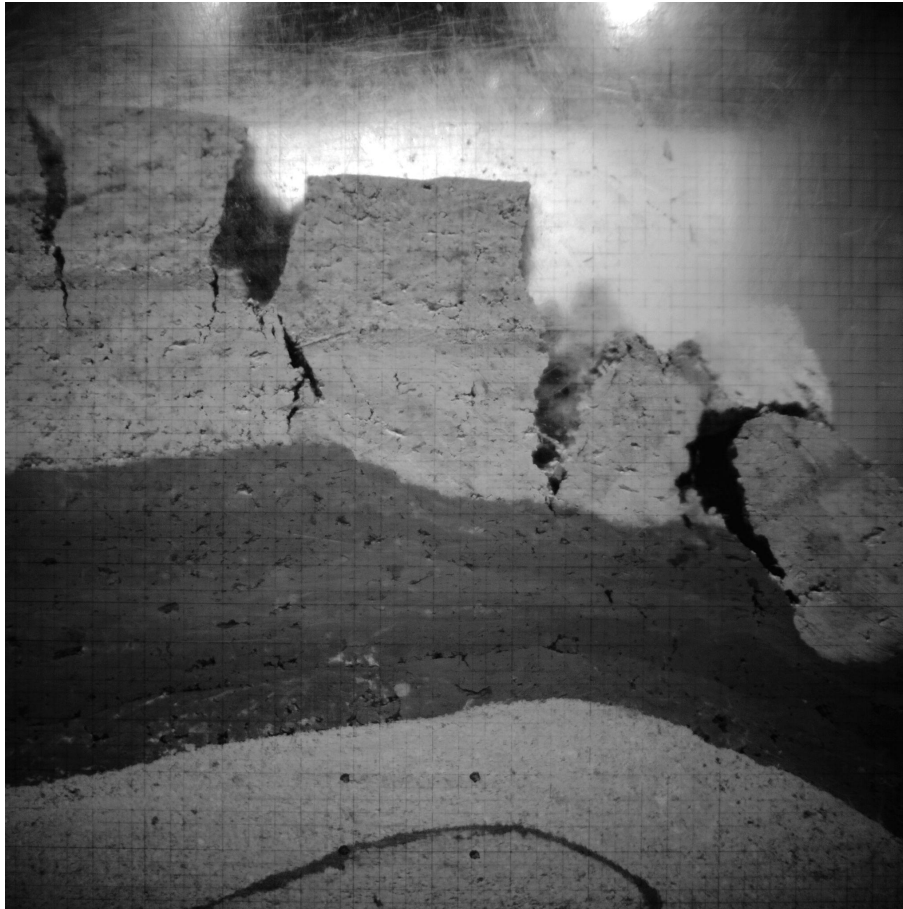


Figure 31. Whole sliding, breaking up and collapsing.

A huge deep-seated ancient rock landslide

M. G. Tang et al.

[Title Page](#)

[Abstract](#)

[Introduction](#)

[Conclusions](#)

[References](#)

[Tables](#)

[Figures](#)

[◀](#)

[▶](#)

[◀](#)

[▶](#)

[Back](#)

[Close](#)

[Full Screen / Esc](#)

[Printer-friendly Version](#)

[Interactive Discussion](#)



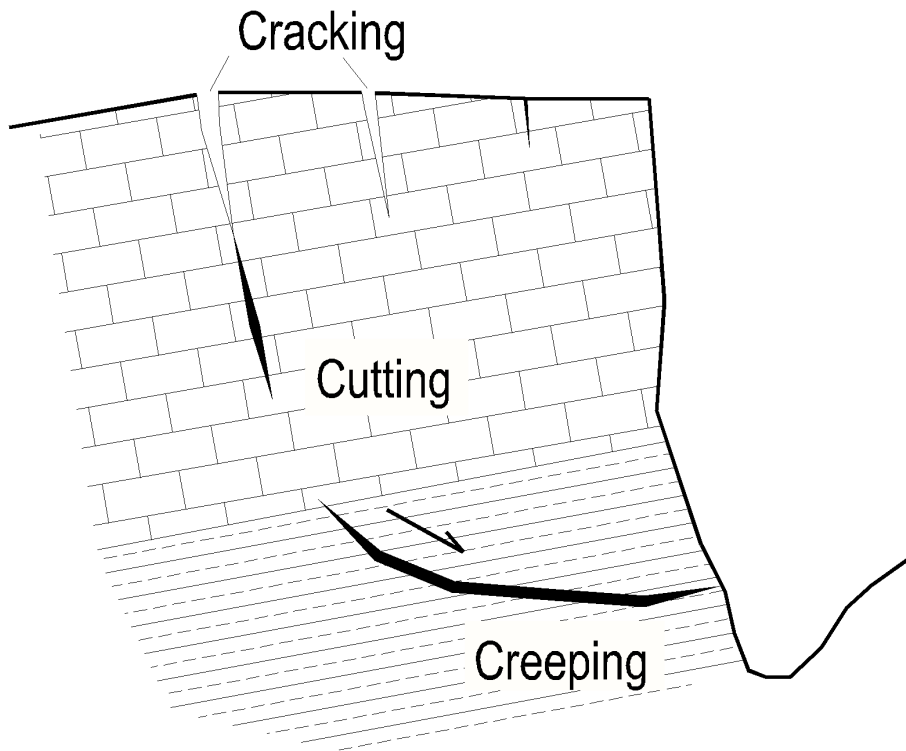


Figure 32. Sketch of failure type of the landslide.

A huge deep-seated ancient rock landslide

M. G. Tang et al.

[Title Page](#)

[Abstract](#)

[Introduction](#)

[Conclusions](#)

[References](#)

[Tables](#)

[Figures](#)

[⏪](#)

[⏩](#)

[⏴](#)

[⏵](#)

[Back](#)

[Close](#)

[Full Screen / Esc](#)

[Printer-friendly Version](#)

[Interactive Discussion](#)





Figure 33. The Chana landslide, Longyangxia, China.

A huge deep-seated ancient rock landslide

M. G. Tang et al.

[Title Page](#)

[Abstract](#)

[Introduction](#)

[Conclusions](#)

[References](#)

[Tables](#)

[Figures](#)

[◀](#)

[▶](#)

[◀](#)

[▶](#)

[Back](#)

[Close](#)

[Full Screen / Esc](#)

[Printer-friendly Version](#)

[Interactive Discussion](#)



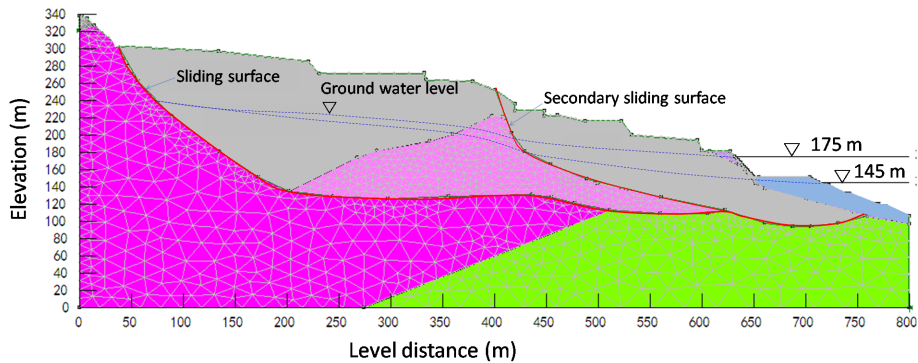


Figure 34. Stability analysis model of the Sanmashan landslide.

A huge deep-seated ancient rock landslide

M. G. Tang et al.

[Title Page](#)

[Abstract](#)

[Introduction](#)

[Conclusions](#)

[References](#)

[Tables](#)

[Figures](#)



[Back](#)

[Close](#)

[Full Screen / Esc](#)

[Printer-friendly Version](#)

[Interactive Discussion](#)



A huge deep-seated ancient rock landslide

M. G. Tang et al.

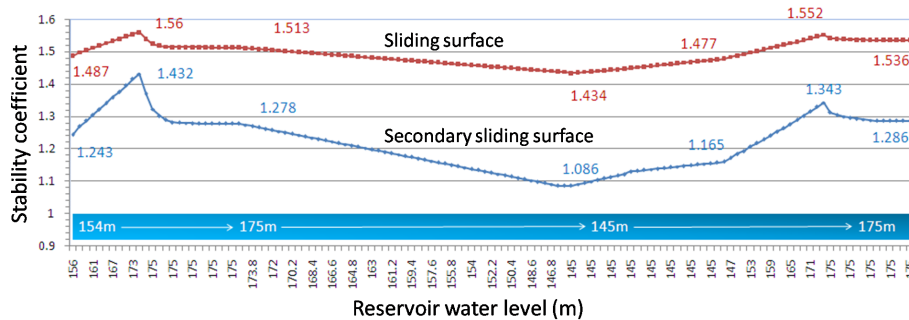


Figure 35. Stability changes with water level of the Three Gorges reservoir.

Title Page

Abstract Introduction

Conclusions References

Tables Figures

⏪ ⏩

◀ ▶

Back Close

Full Screen / Esc

Printer-friendly Version

Interactive Discussion



A huge deep-seated ancient rock landslide

M. G. Tang et al.

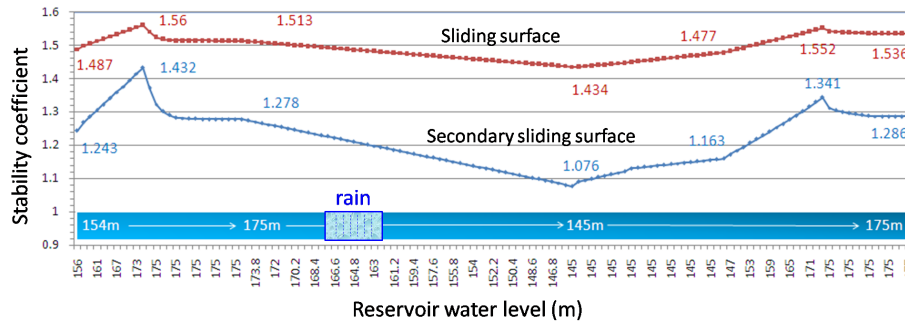


Figure 36. Stability changes with water level of the Three Gorges reservoir and rainfall.

[Title Page](#)

[Abstract](#) [Introduction](#)

[Conclusions](#) [References](#)

[Tables](#) [Figures](#)

[⏪](#) [⏩](#)

[⏴](#) [⏵](#)

[Back](#) [Close](#)

[Full Screen / Esc](#)

[Printer-friendly Version](#)

[Interactive Discussion](#)

